Neuronal signature of an antipsychotic response

Jeffrey Parrilla-Carrero
Department of Neuroscience, Medical University of South Carolina https://orcid.org/0000-0001-9736-8175

Anna Kruyer
Department of Neuroscience, Medical University of South Carolina https://orcid.org/0000-0001-9267-9492

Reda M. Chalhoub
Department of Neuroscience, Medical University of South Carolina https://orcid.org/0000-0001-9774-6359

Courtney Powell
Department of Neuroscience, Medical University of South Carolina

Shanna Resendez
Department of Psychiatry, University of North Carolina at Chapel Hill https://orcid.org/0000-0003-3831-5481

Davide Amato (amatodavide@gmail.com)
Department of Neuroscience, Medical University of South Carolina

Research Article

Keywords: calcium imaging, nucleus accumbens core, medium spiny neurons, sigma receptor, GIRK, synaptic transmission, long-term potentiation, NMDA, antipsychotics, behavior

Posted Date: September 17th, 2020

DOI: https://doi.org/10.21203/rs.3.rs-72975/v1

Neuronal signature of an antipsychotic response

Jeffrey Parrilla-Carrero[1], Anna Kruyer[1], Reda M. Chalhoub[1], Courtney Powell[1], Shanna Resendez[2], Davide Amato[1]

[1]Department of Neuroscience, Medical University of South Carolina, Charleston, SC, USA

[2]Department of Psychiatry, Cell Biology and Physiology, University of North Carolina at Chapel Hill, Chapel Hill, NC, USA

Keywords: calcium imaging, nucleus accumbens core, medium spiny neurons, D1 receptor, D2 receptor, inhibitory post-synaptic current, G protein-coupled inward rectifying potassium channel, synaptic transmission, long-term potentiation, NMDA, antipsychotics, behavior.

Corresponding author:

Dr. Davide Amato

amatod@musc.edu (or amatodavide@gmail.com)

Department of Neuroscience

Medical University of South Carolina

Charleston, SC, USA

Word counts:

Abstract: 154

Text: 2091

References: 45

Abstract

D2 receptor blockade has been cited as a principal mechanism of action of all antipsychotic medications, but is poorly predictive of symptom improvement or neurophysiological responses recorded using human brain imaging. A potential hurdle in interpreting such human imaging studies arises from the inability to distinguish activity within neuronal subcircuits. We used single cell resolution imaging to record activity in distinct populations of medium spiny neurons *in vivo* within the mouse ventral striatum, a structure associated with schizophrenia symptoms and antipsychotic therapeutic efficacy. While we expected the antipsychotic haloperidol to excite D2 receptor expressing neurons, we report a strong cellular depression mediated by the hypofunctional NMDA channel, which may be mediated in part by the action of haloperidol on the sigma1 receptor. Altogether, the impact of haloperidol on Ca^{2+} events in D2 receptor expressing neurons predicted psychomotor inhibition. Our results elucidate mechanisms by which antipsychotics act rapidly in the brain to impact psychomotor outputs.

Antipsychotic drugs (APDs) are widely used to treat psychosis in schizophrenia [1,2] and symptoms in other neuropsychiatric conditions [3]. Blocking dopamine signaling onto 60-80% of striatal D2 receptors (D2r) is thought to underlie their therapeutic efficacy [4,5]. However, studies showing symptom improvement at a broader range of D2r blockade (i.e. 16-95%) [6-10] suggest that this mechanism is poorly predictive of antipsychotic response. Assessment of APD function at a circuit level has proven more predictive of behavioral efficacy in humans [11-13] and rodents [14]. In human patients, the effects of APDs on striatal circuitry are assessed from fMRI BOLD signal, which is inhibited by APDs [11,12]. This clinical response is at odds with expectations, given the physiology of dopamine receptor expressing striatal cells that intracellularly couple to either $G_{i/o}$ (D2r) or $G_{s/o}$ (D1 receptors, D1r), thereby leading to cell inhibition and stimulation, respectively [15,16]. Since APDs are antagonists or inverse agonists of D2r [17], but largely spare D1r, the hyperdopaminergic signaling thought to underlie psychosis shifts to D1r in the presence of APDs, since D2rs are occupied, and the net striatal response is expected to be excitation [15]. Thus, despite the broad clinical application of APDs, the neurobiology underlying their psychomotor effects is unclear and difficult to explain based on mere D2r blockade.

To clarify these mechanisms, we used single cell *in vivo* calcium (Ca^{2+}) imaging to analyze activity of D1r- and D2r-expressing neurons in freely moving mice at baseline and in response to an acute intraperitoneal injection of the typical APD haloperidol (HAL 0.5mg/kg, Fig. 1A), a widely prescribed APD with high affinity for D2r [18]. Striatal cells respond to HAL within minutes [19], contributing to changes in brain structure [20] and symptoms [21] within hours. We determined the earliest psychomotor effects of HAL in relationship with D1r and D2r neuronal responses in the nucleus accumbens core (NAcc), a prominent striatal structure involved in spontaneous locomotion in animals [22,23] and in psychosis and antipsychotic responses in humans [11-13,24].

Because medium spiny neurons (MSNs) are the most prevalent neuronal type in the striatum (~95%) in humans and animals [25] for simplicity we will refer to labeled cells as MSNs throughout the text. We used D1- and D2-cre transgenic mice [26] to obtain selective expression of the Ca^{2+} sensing fluorophore GCaMP6f

in D1- or D2-MSNs (Fig. 1B), recorded with gradient refractive index lenses connected to a head mounted miniature microscope (Fig.1C and methods). We measured Ca^{2+} events from a total of 568 MSNs (246 D1-MSNs and 322 D2-MSNs from 8 mice each) over 45 min (15 min baseline and 30 min after HAL or saline injection (Fig. 1D-E) while animals moved freely in an open field to which they were previously habituated. At baseline D1-MSNs were more active than D2-MSNs (Fig. 2A). In animals that received saline, D1- but not D2-MSN activity correlated positively with locomotion (Fig. S1). An acute injection of HAL did not reduce spontaneous locomotion relative to saline-injected animals (Fig 2B) and did not induce catalepsy, but moderately impacted reward reactivity (Fig S2-3). Within the first 5 min HAL depressed Ca^{2+} events in D2-MSNs compared to their baseline activity (Fig. 2C-D) and compared to saline-injected animals (Fig. S4A) and the reduction was maintained throughout the recording session. Quite the opposite, HAL acutely elevated Ca^{2+} events in D1-MSNs during the first 5 min after injection compared to their baseline activity, although D1-MSN activity was gradually reduced over the course of the recording session (Fig. 2C-D). After HAL injection, D2-MSN activity was positively correlated with locomotion (Fig. 2E). No correlation was found between D1-MSN activity and locomotion after HAL (Fig. 2F). These data suggest that D1-MSN activity may impact motor behavior at baseline, but in the presence of an APD, NAcc D2-MSNs drive spontaneous locomotion.

MSN firing rate is not constant, but alternates between periods of relative silence and episodes of moderate or high firing [27,28]. For this reason, the depression of D2-MSN activity after HAL could result from complete abolition of Ca^{2+} events (i.e. no firing activity) or instead could result from an activity switch from high-to-low firing. We analyzed the cumulative frequency distributions of Ca^{2+} events at baseline and after HAL treatment and found that HAL did not completely suppress Ca^{2+} events, but instead decreased the number of D2- and D1- MSNs firing at high frequency (Fig. 2G-H). By subdividing MSNs into quartiles according to frequency of Ca^{2+} events at baseline, we found that HAL decreased the proportion of D2-MSNs exhibiting high and moderate Ca^{2+} spike frequency gradually over the 30 min recording session, whereas the proportion of D2-MSNs with low or no Ca^{2+} events were ultimately ~80% of all D2-MSNs (Fig. 2I).

No changes in firing frequency were observed in D1-MSNs after HAL during the first 20-min of the recording session, but a significant shift was observed during the last 10 min of recording, where the proportion of cells firing at high frequency was reduced compared to baseline (Fig. 2J). Since NAcc MSN firing is the result of a summation of excitatory and inhibitory inputs [29,30], we compared the increased/decreased ratio of MSN activity for each animal based on the number of neurons firing above or below the median at baseline to estimate the net effect of HAL on MSN activity. Confirming the results in Fig. 2I-J, HAL depressed D2-MSNs (Fig. 2K), but did not impact D1-MSNs (Fig. 2L).

D2r stimulation inhibits adenylate cyclase and cyclic AMP production through $G\alpha_{i/o}$ and endogenous dopamine has ~1000x higher potency for D2r than D1r at baseline [31]. D2r blockade with APDs prevents this tonic inhibition, facilitating D2-MSN excitation [15,32,33]. Furthermore, since HAL is an inverse D2r agonist [17], depression of D2-MSN activity in our study was unexpected. Importantly, at the dose used, HAL does not saturate all D2r [34]. Thus the possibility remains that spared D2r permitted endogenous dopamine to generate inhibitory post-synaptic currents (IPSCs) in NAcc D2-MSNs. To determine if dopamine could elicit IPSCs in NAcc D2-MSNs in HAL treated mice, we overexpressed the G protein-coupled inward rectifying potassium (GIRK2) channel in the NAcc of Drd2-eGFP mice using AAV2/9 -GIRK2-TdTomato (Fig. S5). Because endogenous D2r, but not D1r on MSNs can couple to GIRK2 channels, GIRK2 functions as a sensor providing a rapid, direct readout of IPSC-mediated synaptic D2r activation (D2r-IPSC) [35,36]. As expected, synaptic dopamine stimulation evoked D2r-IPSCs in NAcc D2-MSNs in control animals and HAL reduced it five-fold, (Fig. 3A). The lag to IPSC onset and decay increased after HAL treatment indicating a delayed NAcc D2r-IPSCs (Fig. 3B) and reduced rate of dopamine clearance, respectively (Fig. 3C). Importantly, we estimated that ~21-45% of D2r were spared by HAL depending on incoming dopaminergic transmission, with a more robust D2r-IPSC reduction following increased dopamine transmission. Indeed, HAL suppressed only 44-66% of D2r-IPSC at low intensity stimulation and 76-81% at higher stimulation (Fig. 3D).

Together, these data indicate that HAL effectively reduced post-synaptic dopamine signaling onto NAcc D2-MSNs, but also that endogenous dopamine could stimulate a pool of spared NAcc D2r even in the presence of HAL. The reduced D2r-IPSC decay indicates reduced dopamine clearance, which could prolong dopamine transmission onto both MSN subtypes (Fig. 2C-D). While we recapitulated previous reports on partial receptor occupancy [14,34] and dopamine uptake blockade [14] after systemic HAL treatment, we show that post-synaptic D2r blockade cannot explain the depression of NAcc D2-MSN activity, suggesting that other mechanisms are likely to be involved in the HAL-induced suppression of D2-MSNs *in vivo.*

The decrease in Ca^{2+} conductance may derive not only from decreased D2-IPSCs [37], but also from alterations in pre- and post-synaptic excitatory transmission. NAcc glutamatergic terminals express D2r [38] and HAL functionally competes with endogenous dopamine for binding [39]. Because our conditions fall short of D2r saturation, it is possible that stimulation of spared D2r by dopamine could have reduced NAcc glutamate release [30]. To test this hypothesis, we conducted *ex vivo* whole-cell electrophysiological recordings from NAcc D2-MSNs in control and HAL treated mice. We first determined whether glutamate release probability was altered by HAL using the paired-pulse ratio (PPR) of evoked excitatory postsynaptic currents (EPSCs). PPR was significantly reduced on D2-MSNs of HAL treated mice (Fig. 4A), excluding that reduced excitatory transmission onto D2-MSNs contributed to D2-MSN suppression after HAL. Next, we evaluated putative post-synaptic alterations by measuring the ratio of α -amino-3-hydroxy-5-methyl-4-isoxazolepropionic acid receptors (AMPArs) and N-methyl-D-aspartate receptors (NMDArs). Pharmacological isolation of AMPAr and NMDAr currents revealed an enhanced AMPAr/NMDAr in D2-MSNs in HAL treated mice (Fig. 4B). While increased AMPAr/NMDAr may broadly indicate enhanced synaptic strength (i.e. long-term potentiation, LTP) in D2-MSNs, an imbalanced AMPAr/NMDAr could also result from decreased NMDAr rather than increased AMPAr currents, which is likely to reduce synaptic strength.

To determine whether a systemic HAL injection modified NMDAr currents, we examined the current-voltage (I/V) relationship of pharmacologically isolated NMDAr currents in D2-MSNs. NMDAr I/V curves

in D2-MSNs were significantly decreased in HAL treated mice at -20 mV compare to control (Fig. 4C), suggesting that NMDArs undergo gross changes in voltage dependence. Moreover, the NMDAr current at +40 mV revealed faster decay kinetics in mice treated with HAL (Fig. 4D), independently of differences in membrane properties, as membrane capacitance and input resistance did not differ between treatment groups (Table S2). To confirm that HAL facilitated presynaptic, but depressed post-synaptic excitatory transmission we assessed spontaneous EPSC (sEPSC) frequency and amplitude and found that D2-MSNs in HAL treated mice showed a significant increase in sEPSC frequency, but not amplitude (Fig. 4E).

HAL is a potent inhibitor of the sigma receptor [40] , which is known to regulate pre- and post-synaptic glutamate transmission [41,42]. To test if HAL altered NMDA receptor function by blocking the sigma receptor we bath applied the sigma receptor agonist siramisine and found that while siramisine significantly decreased NMDA current in D2-MSNs of control animals, this effect was antagonized in HAL-treated animal (Fig.4F). Together, these findings show that HAL alters NMDA excitatory transmission likely through blockade of sigma receptor function, likely leading to alterations in synaptic plasticity. Because synaptic plasticity relies on Ca^{2+} influx through NMDAr [43] we expected that the impact of HAL on NMDAr function would alter synaptic plasticity within the striatal network. To determine whether decreased NMDAr function after HAL altered the signature of synaptic plasticity, we measured the amplitude of field EPSPs after the application of high-frequency stimulation (HFS) of glutamatergic afferent fibers in the NAcc. In normal conditions the application of HFS enables Ca^{2+} entry through post-synaptic NMDAr and triggers NMDAr-dependent LTP [43]. Accordingly, the amplitudes of field EPSPs were significantly increased from control mice (Fig. 4E) after HFS. To examine whether this LTP was mediated by NMDAR activation, field EPSPs were recorded in the presence of the selective NMDAR antagonist D-AP5, which inhibited synaptic strength expression (Fig. 4E) and confirmed the NMDAR-dependency of LTP. Since HAL shortened NMDAr decay kinetics, thereby reducing the amount of Ca^{2+} entry through NMDAr, we predicted that LTP magnitude in the NAcc would be reduced by HAL. Indeed, as shown in (Fig. 4F-G), application of HFS decreased field EPSP amplitude below baseline after HAL, demonstrating that the same

protocol that potentiated synaptic transmission in control animals, instead depressed synaptic transmission in mice receiving HAL.

We reveal for the first time rapid neuronal responses of an antipsychotic in relationship to psychomotor output, which is largely independent of D2 receptor blockade. Importantly, locomotion was correlated with NAcc D2-MSNs Ca^{2+} activity after HAL. The suppression of Ca^{2+} events in NAcc D2-MSNs were underlined by shortened NMDAr offset, by antagonism of the sigma receptor and impaired LTP. Paradoxically, these physiological effects emerged despite HAL efficiently blocking dopamine transmission onto ~73% of D2r, minimizing the role of D2r blockade in an antipsychotic response. Because HAL reduced D2-IPSCs without suppressing them completely, our findings suggest that spared D2r might also have mediated the reduced Ca^{2+} signaling and LTP expression. These rapid changes in D2-MSN functional plasticity rather than D2r blockade are likely to contribute to rapid symptom improvements [21,44].

Finally, the depression of MSN responses illuminates the neurobiology underlying reduced striatal BOLD signals observed in human studies coincident with antipsychotic efficacy [11-13]. Here we extend these fMRI studies by showing divergent D1- and D2- MSN responses to an APD, a cell-type signature that cannot be captured by fMRI. Importantly, because in our study a main mechanism of action of HAL was to induce synaptic meta-plasticity by blocking LTP induction, our results shed light on why antipsychotic responses can endure even after treatment discontinuation in humans [45] and animals (Fig. S3).

Acknowledgements

We thank Mr. Eric Dereschewitz for assistance, Mr. Brandon Hughes for making available a proportion of D2-eGFP mice, and Dr. Christopher Ford for donating the GIRK2 virus. We also thank Dr. Peter Kalivas for MATLAB codes and both Dr. Kalivas and Dr. Tom Jhou for lab space. Funding: D.A. and the entire study were supported by Deutsche Forschungsgemeinschaft (AM 488 /1-1/-2) and the Brain & Behavior Research Foundation. J.P.C. was supported by the NIH (DA037327 award to Dr. Tom Jhou). Author contributions: D.A. designed and performed the Ca^{2+} imaging study with input from S.R. D.A. processed

imaging data with help from R.M.C. and input from A.K. J.P.C. and D.A. designed the electrophysiology studies and J.P.C. performed and analyzed the electrophysiology experiments. C.P. conducted catalepsy and reward testing. D.A. drafted the manuscript with contributions from J.P.C. and A.K. and all authors edited the final version of the manuscript. Competing interests: The authors declare no competing interests. Data and materials availability: All experimental data are available in the main text or within the supplement.

References

1 Amato, D., Kruyer, A., Samaha, A. N. & Heinz, A. Hypofunctional Dopamine Uptake and Antipsychotic Treatment-Resistant Schizophrenia. *Frontiers in psychiatry* **10**, 314, doi:10.3389/fpsyt.2019.00314 (2019).

2 Amato, D., Vernon, A. C. & Papaleo, F. Dopamine, the antipsychotic molecule: A perspective on mechanisms underlying antipsychotic response variability. *Neuroscience and biobehavioral reviews* **85**, 146-159, doi:10.1016/j.neubiorev.2017.09.027 (2018).

3 Mark, T. L. For what diagnoses are psychotropic medications being prescribed?: a nationally representative survey of physicians. *CNS drugs* **24**, 319-326, doi:10.2165/11533120-000000000-00000 (2010).

4 Farde, L. *et al.* Positron emission tomographic analysis of central D1 and D2 dopamine receptor occupancy in patients treated with classical neuroleptics and clozapine. Relation to extrapyramidal side effects. *Archives of general psychiatry* **49**, 538-544 (1992).

5 Nordstrom, A. L. *et al.* Central D2-dopamine receptor occupancy in relation to antipsychotic drug effects: a double-blind PET study of schizophrenic patients. *Biological psychiatry* **33**, 227-235 (1993).

6 Kapur, S. *et al.* 5-HT2 and D2 receptor occupancy of olanzapine in schizophrenia: a PET investigation. *The American journal of psychiatry* **155**, 921-928 (1998).

7 Tauscher, J. *et al.* In vivo 123I IBZM SPECT imaging of striatal dopamine-2 receptor occupancy in schizophrenic patients treated with olanzapine in comparison to clozapine and haloperidol. *Psychopharmacology* **141**, 175-181, doi:10.1007/s002130050822 (1999).

8 Bernardo, M. *et al.* Double-blind olanzapine vs. haloperidol D2 dopamine receptor blockade in schizophrenic patients: a baseline-endpoint. *Psychiatry research* **107**, 87-97, doi:10.1016/s0925-4927(01)00085-3 (2001).

9 Vernaleken, I. *et al.* High striatal occupancy of D2-like dopamine receptors by amisulpride in the brain of patients with schizophrenia. *The international journal of neuropsychopharmacology / official scientific journal of the Collegium Internationale Neuropsychopharmacologicum* **7**, 421-430, doi:10.1017/S1461145704004353 (2004).

10 Yokoi, F. *et al.* Dopamine D2 and D3 receptor occupancy in normal humans treated with the antipsychotic drug aripiprazole (OPC 14597): a study using positron emission tomography and [11C]raclopride. *Neuropsychopharmacology : official publication of the American College of Neuropsychopharmacology* **27**, 248-259, doi:10.1016/S0893-133X(02)00304-4 (2002).

11 Sarpal, D. K. *et al.* Antipsychotic treatment and functional connectivity of the striatum in first-episode schizophrenia. *JAMA Psychiatry* **72**, 5-13, doi:10.1001/jamapsychiatry.2014.1734 (2015).

12 Juckel, G. *et al.* Dysfunction of ventral striatal reward prediction in schizophrenic patients treated with typical, not atypical, neuroleptics. *Psychopharmacology* **187**, 222-228, doi:10.1007/s00213-006-0405-4 (2006).

13 Nielsen, M. O. *et al.* Improvement of brain reward abnormalities by antipsychotic monotherapy in schizophrenia. *Archives of general psychiatry* **69**, 1195-1204, doi:10.1001/archgenpsychiatry.2012.847 (2012).

14 Amato, D. *et al.* A dopaminergic mechanism of antipsychotic drug efficacy, failure, and failure reversal: the role of the dopamine transporter. *Molecular psychiatry* (2018).

15 Stoof, J. C. & Kebabian, J. W. Opposing roles for D-1 and D-2 dopamine receptors in efflux of cyclic AMP from rat neostriatum. *Nature* **294**, 366-368, doi:10.1038/294366a0 (1981).

16 Bateup, H. S. *et al.* Distinct subclasses of medium spiny neurons differentially regulate striatal motor behaviors. *Proceedings of the National Academy of Sciences of the United States of America* **107**, 14845-14850, doi:10.1073/pnas.1009874107 (2010).
17 Hall, D. A. & Strange, P. G. Evidence that antipsychotic drugs are inverse agonists at D2 dopamine receptors. *British journal of pharmacology* **121**, 731-736, doi:10.1038/sj.bjp.0701196 (1997).
18 McCormick, P. N. *et al.* The antipsychotics olanzapine, risperidone, clozapine, and haloperidol are D2-selective ex vivo but not in vitro. *Neuropsychopharmacology : official publication of the American College of Neuropsychopharmacology* **35**, 1826-1835, doi:10.1038/npp.2010.50 (2010).
19 Pozzi, L. *et al.* Opposite regulation by typical and atypical anti-psychotics of ERK1/2, CREB and Elk-1 phosphorylation in mouse dorsal striatum. *Journal of neurochemistry* **86**, 451-459, doi:10.1046/j.1471-4159.2003.01851.x (2003).
20 Tost, H. *et al.* Acute D2 receptor blockade induces rapid, reversible remodeling in human cortical-striatal circuits. *Nature neuroscience* **13**, 920-922, doi:10.1038/nn.2572 (2010).
21 Kapur, S. *et al.* Evidence for onset of antipsychotic effects within the first 24 hours of treatment. *The American journal of psychiatry* **162**, 939-946, doi:10.1176/appi.ajp.162.5.939 (2005).
22 Kelley, A. E., Gauthier, A. M. & Lang, C. G. Amphetamine microinjections into distinct striatal subregions cause dissociable effects on motor and ingestive behavior. *Behavioural brain research* **35**, 27-39, doi:10.1016/s0166-4328(89)80005-1 (1989).
23 Boye, S. M., Grant, R. J. & Clarke, P. B. Disruption of dopaminergic neurotransmission in nucleus accumbens core inhibits the locomotor stimulant effects of nicotine and D-amphetamine in rats. *Neuropharmacology* **40**, 792-805, doi:10.1016/s0028-3908(01)00003-x (2001).
24 Wadenberg, M. L., Ericson, E., Magnusson, O. & Ahlenius, S. Suppression of conditioned avoidance behavior by the local application of (-)sulpiride into the ventral, but not the dorsal, striatum of the rat. *Biological psychiatry* **28**, 297-307, doi:10.1016/0006-3223(90)90657-n (1990).
25 Graveland, G. A., Williams, R. S. & DiFiglia, M. A Golgi study of the human neostriatum: neurons and afferent fibers. *J Comp Neurol* **234**, 317-333, doi:10.1002/cne.902340304 (1985).
26 Gerfen, C. R., Paletzki, R. & Heintz, N. GENSAT BAC cre-recombinase driver lines to study the functional organization of cerebral cortical and basal ganglia circuits. *Neuron* **80**, 1368-1383, doi:10.1016/j.neuron.2013.10.016 (2013).
27 Wilson, C. J. Predicting the response of striatal spiny neurons to sinusoidal input. *Journal of neurophysiology* **118**, 855-873, doi:10.1152/jn.00143.2017 (2017).
28 Beatty, J. A., Song, S. C. & Wilson, C. J. Cell-type-specific resonances shape the responses of striatal neurons to synaptic input. *Journal of neurophysiology* **113**, 688-700, doi:10.1152/jn.00827.2014 (2015).
29 Wilson, C. J. & Kawaguchi, Y. The origins of two-state spontaneous membrane potential fluctuations of neostriatal spiny neurons. *The Journal of neuroscience : the official journal of the Society for Neuroscience* **16**, 2397-2410 (1996).
30 Wang, W. *et al.* Regulation of prefrontal excitatory neurotransmission by dopamine in the nucleus accumbens core. *The Journal of physiology* **590**, 3743-3769, doi:10.1113/jphysiol.2012.235200 (2012).
31 Kebabian, J. W. & Calne, D. B. Multiple receptors for dopamine. *Nature* **277**, 93-96, doi:10.1038/277093a0 (1979).
32 Svenningsson, P. *et al.* Regulation of the phosphorylation of the dopamine- and cAMP-regulated phosphoprotein of 32 kDa in vivo by dopamine D1, dopamine D2, and adenosine A2A receptors.

Proceedings of the National Academy of Sciences of the United States of America **97**, 1856-1860, doi:10.1073/pnas.97.4.1856 (2000).

33 Yapo, C. *et al.* Detection of phasic dopamine by D1 and D2 striatal medium spiny neurons. *The Journal of physiology* **595**, 7451-7475, doi:10.1113/JP274475 (2017).

34 Kapur, S., Wadenberg, M. L. & Remington, G. Are animal studies of antipsychotics appropriately dosed? Lessons from the bedside to the bench. *Canadian journal of psychiatry. Revue canadienne de psychiatrie* **45**, 241-246, doi:10.1177/070674370004500302 (2000).

35 Marcott, P. F., Mamaligas, A. A. & Ford, C. P. Phasic dopamine release drives rapid activation of striatal D2-receptors. *Neuron* **84**, 164-176, doi:10.1016/j.neuron.2014.08.058 (2014).

36 Marcott, P. F. *et al.* Regional Heterogeneity of D2-Receptor Signaling in the Dorsal Striatum and Nucleus Accumbens. *Neuron* **98**, 575-587 e574, doi:10.1016/j.neuron.2018.03.038 (2018).

37 Hu, X. T., Dong, Y., Zhang, X. F. & White, F. J. Dopamine D2 receptor-activated Ca2+ signaling modulates voltage-sensitive sodium currents in rat nucleus accumbens neurons. *Journal of neurophysiology* **93**, 1406-1417, doi:10.1152/jn.00771.2004 (2005).

38 Wang, H. & Pickel, V. M. Dopamine D2 receptors are present in prefrontal cortical afferents and their targets in patches of the rat caudate-putamen nucleus. *J Comp Neurol* **442**, 392-404, doi:10.1002/cne.10086 (2002).

39 Seeman, P., Chau-Wong, M., Tedesco, J. & Wong, K. Brain receptors for antipsychotic drugs and dopamine: direct binding assays. *Proceedings of the National Academy of Sciences of the United States of America* **72**, 4376-4380, doi:10.1073/pnas.72.11.4376 (1975).

40 Tam, S. W. & Cook, L. Sigma opiates and certain antipsychotic drugs mutually inhibit (+)-[3H] SKF 10,047 and [3H]haloperidol binding in guinea pig brain membranes. *Proceedings of the National Academy of Sciences of the United States of America* **81**, 5618-5621, doi:10.1073/pnas.81.17.5618 (1984).

41 Klawonn, A. M. *et al.* The Sigma-2 Receptor Selective Agonist Siramesine (Lu 28-179) Decreases Cocaine-Reinforced Pavlovian Learning and Alters Glutamatergic and Dopaminergic Input to the Striatum. *Front Pharmacol* **8**, 714, doi:10.3389/fphar.2017.00714 (2017).

42 Pabba, M. The essential roles of protein-protein interaction in sigma-1 receptor functions. *Front Cell Neurosci* **7**, 50, doi:10.3389/fncel.2013.00050 (2013).

43 Artola, A. & Singer, W. Long-term depression of excitatory synaptic transmission and its relationship to long-term potentiation. *Trends in neurosciences* **16**, 480-487, doi:10.1016/0166-2236(93)90081-v (1993).

44 Agid, O., Kapur, S., Arenovich, T. & Zipursky, R. B. Delayed-onset hypothesis of antipsychotic action: a hypothesis tested and rejected. *Archives of general psychiatry* **60**, 1228-1235, doi:10.1001/archpsyc.60.12.1228 (2003).

45 Nyberg, S., Farde, L. & Halldin, C. Delayed normalization of central D2 dopamine receptor availability after discontinuation of haloperidol decanoate. Preliminary findings. *Archives of general psychiatry* **54**, 953-958 (1997).

Figures

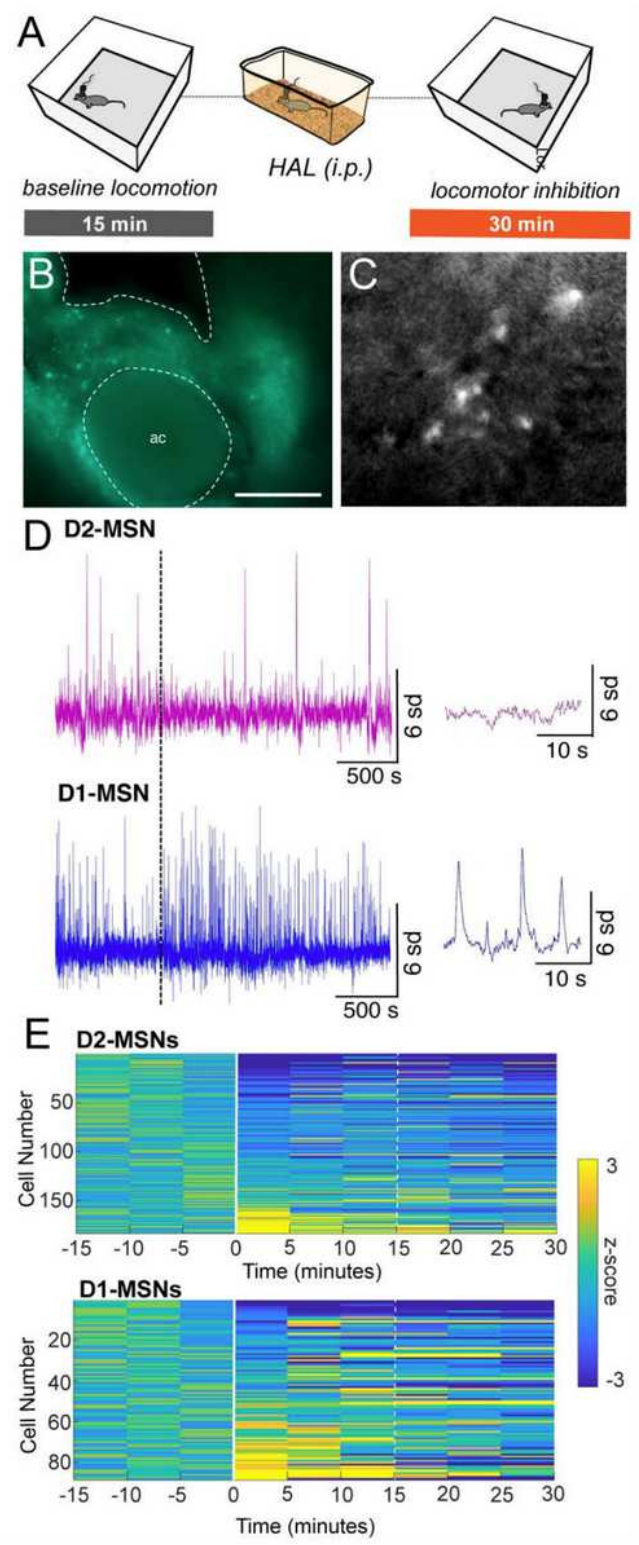

Figure 1

In vivo Ca2+ imaging of D2- and D1-MSNs in the nucleus accumbens core in response to the antipsychotic haloperidol. (A) Schematic of the study. (B) Representative GCaMP6f expression in nucleus accumbens core MSNs (dashed line shows lens placement and ac, anterior commissure; scale=200 μm).

(C) Representative GCaMP6f signal in a D2rd2-cre mouse. (D) Representative traces from a D2- and a D1-MSN at baseline and after an i.p. injection of haloperidol (dashed line). Right panel shows magnified signal ~5 min after haloperidol injection. (E) Heat maps show D2- and D1-MSN activity as z-scores at baseline (-15 to 0 min) and after acute haloperidol (0-30 min).

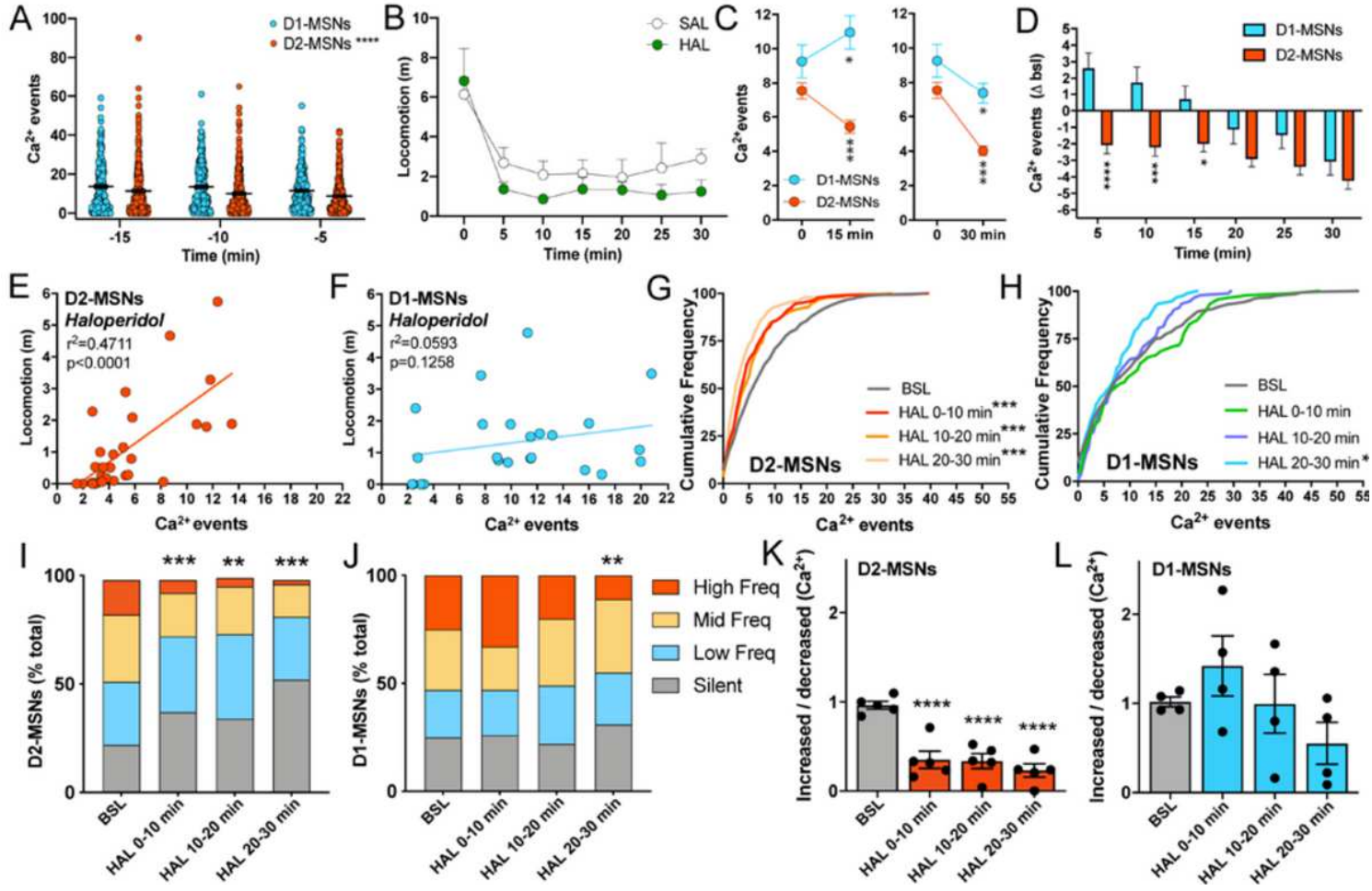

Figure 2

Haloperidol suppresses D2-MSNs. (A) D1-MSNs were more active than D2-MSNs at baseline (BSL, 2-way ANOVA, F(1.570,386.2)=25.62, p<0.0001). (B) An acute haloperidol injection (HAL) did not reduced spontaneous locomotion relative to saline-injected animals (SAL; 2-way ANOVA, F(1,121)=2.084, p=0.1514). (C-D) Haloperidol reduced Ca2+ events in D2-MSNs (C left, 15-min after acute haloperidol vs. last 5-min baseline, 2-way ANOVA F(1,277)=18.78, p<0.0001 treatment x MSN response; right, last 15-min recording vs. last 5-min BSL, 2-way ANOVA F(1,277)= 14.38). Haloperidol increased Ca2+ events in D1-MSNs by 15 min, but ultimately suppressed them (D, 2-way ANOVA F(5,1385)=7.302 p<0.0001 treatment x MSN response). (E) D2-MSN activity correlated positively with spontaneous locomotion after haloperidol (r^2=0.4711, p<0.0001). (F) No correlation in D1-MSNs (r^2=0.0593, p=0.1258). Frequency distributions show Ca2+ events in D2- (G, ***p<0.001 vs BSL using Kolmogorov Smirnov) and D1-MSNs (H, *p<0.05 vs BSL using Kolmogorov Smirnov). D2- (I) and D1-MSNs (J) were grouped according to firing frequency at BSL, where quartiles were defined as silent (0-2 Ca2+ events), low frequency (3-6 events), mid frequency (7-15 events), and high frequency (16+ events). Haloperidol increased the proportion of

silent D2-MSNs and reduced high frequency firing. (I, **p<0.01 vs BSL, ***p<0.001 vs BSL using Chi^2). After 20min, D1-MSNs also exhibited a shift toward reduced high frequency firing (J, **p<0.01 vs BSL using Chi^2). (K-L) A ratio of increased/decreased cellular activity compares number of cells above (increased) or below (decreased) the median at BSL for each animal. A greater proportion of D2-MSNs were decreased by haloperidol, resulting in a reduction in this ratio throughout recording (K, 1-way ANOVA F(3,12)=34.75 p<0.0001). There was no impact of haloperidol on this metric in D1-MSNs (L, 1-way ANOVA F(3,9)=2.44 p=0.1305). *p<0.05, **p<0.01, ***p<0.001, ****p<0.0001 using Sidak's test.

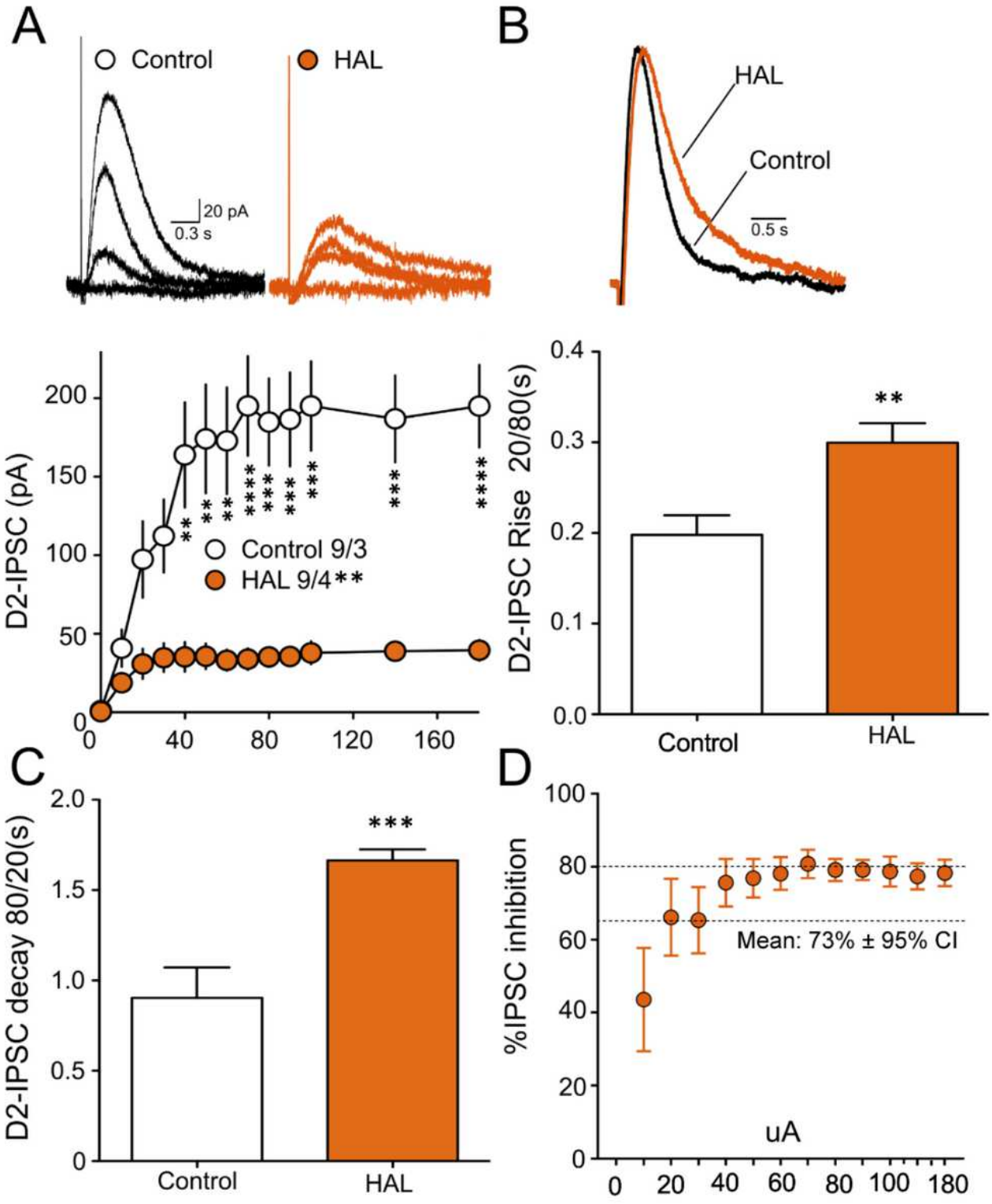

Figure 3

D2r-dependent IPSCs in D2-MSNs. (A) Haloperidol attenuated D2r-IPSCs (2-way ANOVA F(1,12)=13.86 **p=0.0029; **p<0.01, ***p<0.001, ****p<0.0001 vs control using Sidak'stest). (B) Haloperidol increased IPSC rise (t(16)=3.338, **p<0.0021) and (C) decay (t(16)=4.249, ***p<0.0003). (D) Haloperidol suppressed 44-66% of D2r-IPSC at low intensity stimulation (i.e. 10-30 μA) and 76-81% at higher stimulation (i.e. 40-180 μA). N=cells/mice.

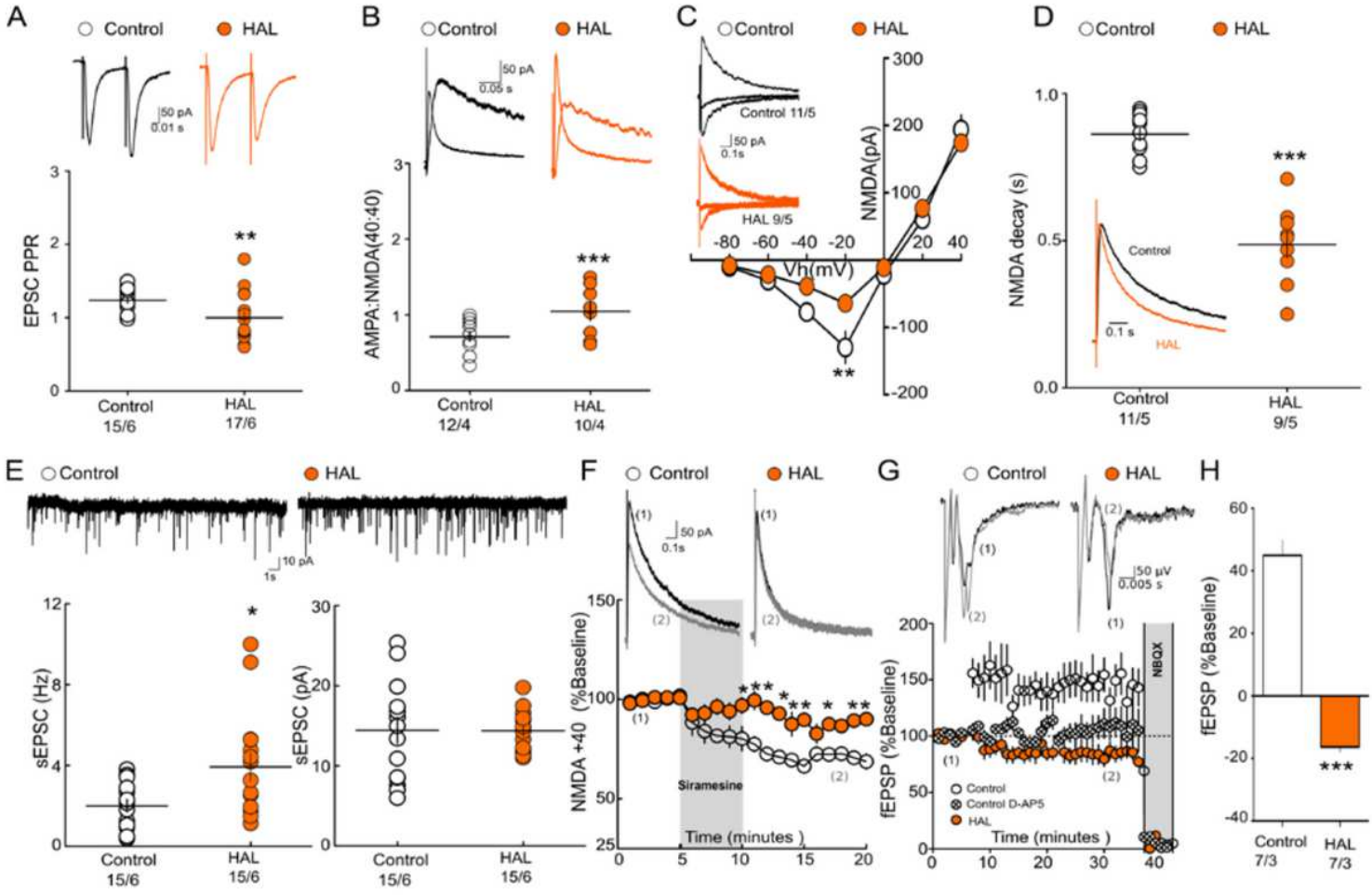

Figure 4

Haloperidol impaired NMDAr-dependent LTP in D2-MSNs. (A) Haloperidol (HAL) reduced PPR evoked EPSCs (t(28)=2.46, *p<0.0102). (B) Pharmacological isolation of AMPAr and NMDAr currents showed an increase in AMPAr:NMDAr after HAL (t(18)=2.676, **p<0.0077). (C) NMDA I/V curves significantly differed after HAL (treatment, 2-way ANOVA F(1,18)=9.42, p=0.0066, at -20mV t(6, 108)=4.096, p=0.001). (D) NMDA current decayed faster after haloperidol (t(18)=8.090, ***p<0.0001). (E) Haloperidol increased sEPSC frequency (left, t(14)=2.46 *p<0.0276), but not sEPSC amplitude (right, t(28)=0.039 *p=0.97). (F) Sigma receptor agonist siramesine (5uM) reduced NMDA receptor currents after HAL (treatment, 2-way ANOVA F(1,7)=17.9, p=0.0039). (G-H) High frequency stimulation increased field EPSPs in controls, but not in HAL-treated mice (G, (t(20)=4.921, ****p<0.0001; H, 2-way ANOVA F(2,490)=26.88, p<0.0001). N=cells/mice

Supplementary Files

This is a list of supplementary files associated with this preprint. Click to download.

- ParrillaCarreroetal.supplement.figures.tables.refs.pdf
- ParrillaCarreroetal.SupplfilewithMaterialandMethods.pdf